*Journal of Applied Electrochemistry* **29**: 1347–1350, 1999.



*Short communication*

# Catalysis of oxygen evolution on $IrO_x$/Pb anodes in acidic sulfate electrolytes for zinc electrowinning

C. LE PAPE-RÉROLLE[1], M.A. PETIT[2] and R. WIART[1]
[1]*UPR 15 du CNRS, Physique des Liquides et Électrochimie, Université Pierre et Marie Curie, Tour 22, 4 Place Jussieu, 75252 Paris Cedex 05, France;*
[2]*Laboratoire d'Environnement et de Chimie Analytique, ERS 657 du CNRS, École Supérieure de Physique et Chimie Industrielles, 10 Rue Vauquelin, 75231 Paris Cedex 05, France*

Received 27 July 1998; accepted in revised form 26 January 1999

*Key words:* electrocatalysis, $IrO_x$ films, lead anodes, zinc electrowinning

## 1. Introduction

Lead alloyed with less than 1% Ag is commonly used as an anode for zinc electrowinning. Lead–silver alloys allow a decrease in the oxygen overpotential, a reduced corrosion rate of lead and an increased mechanical resistance of the material [1–3]. In addition to the oxygen reaction, several oxidation reactions also take place on the lead anodes, which generate complexed $Mn^{3+}$ and $MnO_4^-$ ions in the electrolyte, and $MnO_2$ in the whole cell where slimes are observed to deposit progressively [4–6].

Iridium oxide films have attracted much attention over the last two decades, especially for their high electrocatalytic activity for oxygen evolution [7–10]. Iridium oxide films thermally deposited on titanium are particularly remarkable for their anodic stability and electrocatalytic activity [11–17].

With a view to obtaining similar catalytic effects on the lead anodes for zinc electrowinning, the deposition of iridium oxide on lead surfaces has been attempted. In the present work, the idea was to try to improve the performances of the industrial lead anodes utilized by Union Miniére. The usual deposition of $IrO_x$ by pyrolisis of gels or iridium chloride could not be carried out as the lead substrates are deficient in mechanical resistance at annealing temperatures over 300 °C. Therefore we focused on the various electrochemical procedures of $IrO_x$ deposition which have been previously described [18–23]. Methods giving $IrO_x$ films on cathodes [18, 19] were ruled out as they also produce inclusions of iridium metal corroding rapidly in sulfuric acid media [20]. Alternative methods with anodic $IrO_x$ deposition were preferred [21–23]. Recently, we presented an electrochemical procedure leading to $IrO_x$ films by oxidation of soluble species in basic aqueous solution [23]. Initially formed on conducting $SnO_2$-coated glass electrodes, the $IrO_x$ films can also be deposited on other electrode materials. In this paper, we describe the method of depositing $IrO_x$ on lead substrates, and we present the catalytic properties of these electrodes for oxygen evolution in the electrolyte for zinc electrowinning.

## 2. Preparation and characterization of $IrO_x$ deposits

### 2.1. *Solution for $IrO_x$ deposition*

Chemicals from Aldrich were used as-received. The iridium containing solution for the $IrO_x$ deposition was prepared as follows:

To 0.2 mmol of $K_3IrCl_6$ (104 mg) dissolved in approximately 30 ml of water, 1 mmol of oxalic acid $H_2C_2O_4.2H_2O$ (125 mg) was added. The pH of the solution was raised to 10 by adding 5 mmol of $K_2CO_3$ (690 mg). Due to this increase of pH, the colour of the solution turned from pale yellow to pale green. The volume of the solution was then increased to 50 ml. These freshly prepared solutions are inefficient at iridium oxide deposition. It is necessary to age the iridium solution in air, the shortest ageing time being determined as four days at 35 °C, or 1 day at 45 °C. The ageing is easily controlled by monitoring the absorbance of the solution at 570 nm, which was found to increase linearly from zero. Empirically, we noticed that all solutions found to be efficient at anodic $IrO_x$ deposition have an absorbance at this wavelength which typically exceeds 0.2 (optical cell of pathlength 1 cm). Though this behavior remains unclear, the measurement of the absorbance at 570 nm is the most convenient method of predicting the efficiency of aged solutions for $IrO_x$ deposition.

Efficient solutions can be stored for several weeks at 4 °C without degradation.

### 2.2. *Electrochemical set-up for $IrO_x$ deposition*

A conventional electrochemical set-up was used with the counter and reference electrodes being, respectively, a platinum wire and a saturated mercurous sulfate electrode (SSE: 0.614 V vs SHE). Three kinds of material

were taken as working electrodes, each of area approximately 1 $cm^2$: Pb with 0.0066% Ag, Pb with 0.56% Ag, and Pb covered with a $PbO_2$ layer (generated by oxidizing the Pb surface for 18 h at 1.39 V vs SSE in 1.8 M $H_2SO_4$).

In the described procedure for $IrO_x$ deposition [23], the best $IrO_x$ films on inert electrodes were obtained using a fixed anodic current density of approximately 0.04 mA $cm^{-2}$. Pb electrodes could not be covered by $IrO_x$ under these experimental conditions, as the potential of the anode stabilized at a plateau value of −0.17 V vs SSE which corresponds to the formation of Pb oxides in basic solution. Consequently, the original parameters for $IrO_x$ deposition had to be adjusted to enable the use of Pb electroactive substrates. After several attempts, a potentiostatic method was chosen, which gave regular dark blue films of $IrO_x$ at 0.26 V vs SSE with current densities ranging from 0.1 to 0.3 mA $cm^{-2}$. The charge used for the anodic deposition was limited to 2 C $cm^{-2}$. The Pb electrodes covered with $IrO_x$ were rinsed several times in water and dried at 70 °C. Finally, a thermal treatment at 220 °C for 30 min was carried out in order to stabilize the $IrO_x$ coated surfaces.

### 2.3. *Characterization of $IrO_x$ deposits*

The $IrO_x$ coated surfaces were examined in a scanning electron microscope (SEM) and the Ir content in the electrodes was determined by X-ray energy dispersion spectroscopy (EDS).

The typical morphology of $IrO_x$ deposits, shown in Figure 1, was found to be independent of the three substrates used (Pb, Pb–Ag, or $PbO_2$). Figure 1 reveals that the electrode surface is cracked and nonhomogeneous. The electrode surface may be divided into different regions A, B, and C. The Ir/Pb ratio of each region was determined by EDS and found to decrease from the region A to C, the Ir/Pb ratio of region C being practically that of the substrate. The average value of 38 ± 15% was obtained independently of the three substrates used (Pb, Pb–Ag, or $PbO_2$).

## 3. Catalytic properties for oxygen evolution

The kinetics of the Pb/$IrO_x$ anodes were investigated at 37 °C in the electrolyte for zinc electrowinning, containing 1.83 M $H_2SO_4$, 0.84 M $ZnSO_4$ and 0.091 M $MnSO_4$. The anode and the Al cathode, of equivalent surface areas (1 $cm^2$), were orientated vertically in the cell. Starting from $V = 0.8$ V vs SSE, the polarization curves for $IrO_x$ coated electrodes were obtained by potential steps of 20 mV every 15 min (10 min for the current stabilization and 5 min for the impedance measurements in the frequency range (60 kHz–60 mHz). The high frequency limit of impedance gives the electrolyte resistance, $R_e$, and the potential $E$ corrected for the ohmic drop effect, that is, $E = V - R_e i$, where $i$ denotes the current density.

The polarization curves corresponding to different $IrO_x$ deposits on Pb substrates are shown in Figure 2. Taking into account the limited reproducibility of the curves, it is shown that the anode surface (Pb, Pb–Ag (0.56%) or $PbO_2$) does not significatively influence the catalytic properties of the $IrO_x$ deposit. However, in comparison with the curves obtained in the absence of $IrO_x$ on Pb or Pb–Ag anodes, it clearly appears that the $IrO_x$ deposits act as an electrocatalyst on oxygen evolution in the zinc electrowinning electrolyte: a polarization decrease of at least 340 mV is observed at $i = 50$ mA $cm^{-2}$. It should also be noted, however, that the relative positions of the polarization curves are not connected with the scattered values of the Ir content in the electrodes, as indicated in Figure 2.

Due to the decreased oxygen overpotential, no slimes formed in the electrolyte, which advantageously remained clear with the oxidation of $Mn^{2+}$ into $MnO_4^-$, $Mn^{3+}$ and $MnO_2$ being considerably reduced. In addition, no porous deposit was found on the $IrO_x$ anodes

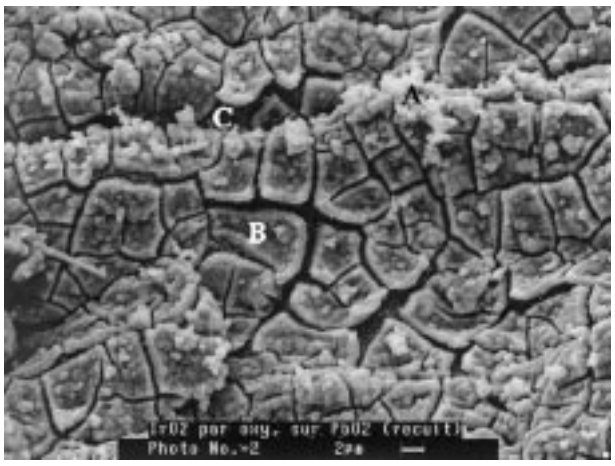


*Fig. 1.* Typical SEM morphology of $IrO_x$ deposit on lead : the Ir/Pb ratio decreases from region A to region C.

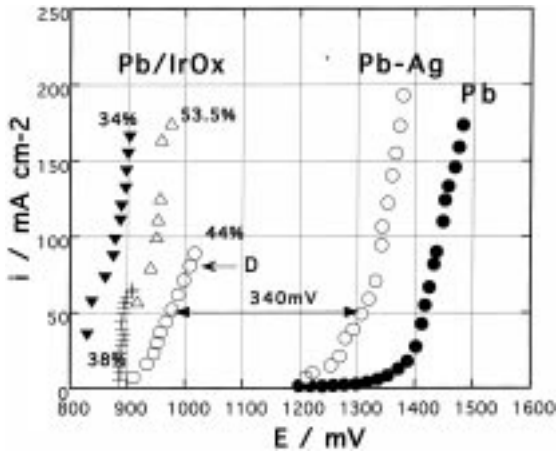


*Fig. 2.* Polarization curves for various anode materials: Pb, Pb–Ag (0.56%), and different $IrO_x$ deposits on Pb. The percentages on curves indicate the Ir content on the surface of the electrodes.


*Fig. 3.* SEM morphology of lead anode covered with $IrO_x$ after use in the zinc electrowinning electrolyte.

during electrolysis (as shown in Figure 3), unlike the experiments performed on Pb–Ag and Pb electrodes [24].

The typical shape of the impedance plots obtained with $IrO_x$ anodes is depicted in Figure 4. The high frequency loop corresponds to the charge transfer resistance, $R_t$, in parallel with the double layer capacitance, $C_{dl}$. A second capacitive loop can also be observed at frequencies close to 1 Hz, but it remains smaller than that of typical Pb–Ag anodes [24]. The charge transfer resistance reflects the catalytic activity of the $IrO_x$ anodes: the $R_t i$ product ranges between 25 and 65 mV, as shown in Figure 5, and those values are much lower than those reported for the Pb–Ag anodes (about 250 mV) [24]. In addition, for all $IrO_x$ electrodes, Figure 5 shows a clear increase of $R_t i$ product with potential. Hence the highest catalytic effect corresponds to the smallest $R_t i$ values, thus indicating that the electrocatalysis is essentially due to an increase in the charge transfer coefficient of the oxygen reaction, in agreement with the already proposed change in the reaction mechanism [25].

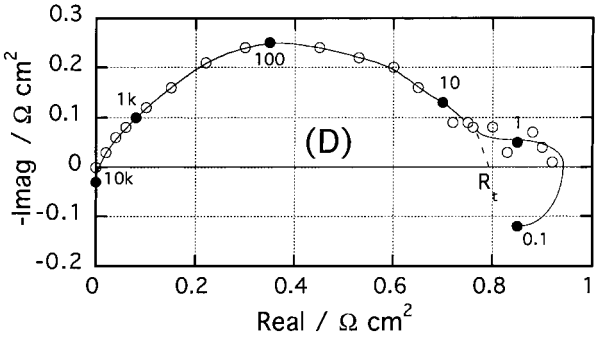


*Fig. 4.* Complex plane impedance plot at point D in Figure 2.

Impedance data also show that the values of the double layer capacitance, $C_{dl}$, of the $IrO_x$ electrodes range between 1 and 10 mF $cm^{-2}$, that is, the same order of magnitude as for the Pb–Ag electrodes [24]. Consequently, the oxygen reaction probably occurs on a

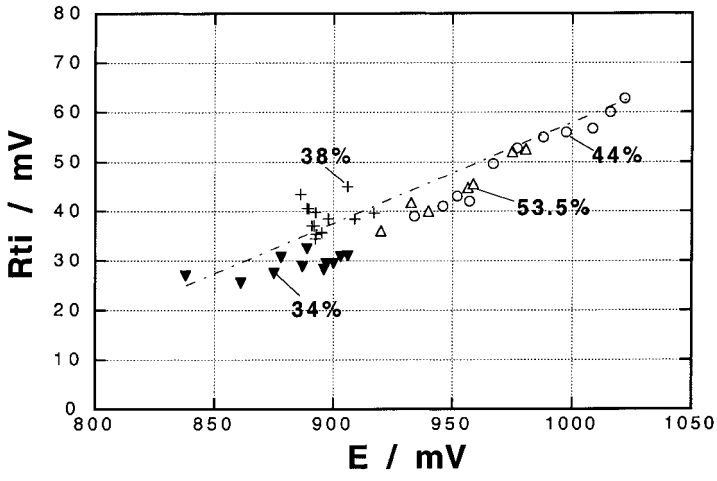


*Fig. 5.* Potential dependencies of the $R_t i$ product corresponding to the curves for the different $IrO_x$ deposits in Figure 2.

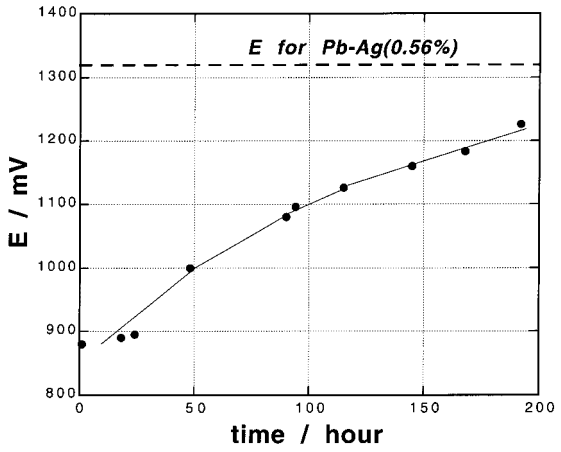


*Fig. 6.* Time dependence of the potential of a lead anode covered with $IrO_x$, at $i = 55$ mA cm$^{-2}$. Dashed line corresponds to a Pb–Ag (0.56%) anode.

large surface area, thus suggesting that the active surface includes not only the external smooth surface visible on Figure 3, but also numerous active sites possibly belonging to a porous sublayer. This question remains entirely unsolved.

To test the catalytic performance of $IrO_x$ deposits over a long time interval, galvanostatic electrolyses were carried out at a current density of 55 mA cm$^{-2}$. As shown in Figure 6, the anode potential slightly increases, and subsequently the energy gain progressively decreases with time. However, after eight days, the electrode potential is still lower (by 100 mV) than that of the Pb–Ag (0.56%) anode. This loss of performance is possibly due to slow dissolution of the $IrO_x$ film.

## 4. Conclusion

$IrO_x$ deposits can be grown on Pb or Pb–Ag substrates by electrochemical oxidation of $IrCl_6^{3-}$. These deposits have been shown to have an electrocatalytic activity on oxygen evolution in the acidic sulfate electrolyte used for zinc electrowinning. This catalytic effect is essentially associated to a stimulation of the transfer coefficient of the reaction.

Tests performed over long time spans reveal a slow loss in catalytic effect during the electrolysis. Improvements in the deposits properties (reproducibility and stability) are expected from the optimization of the conditions of $IrO_x$ deposition and/or of the thermal treatment of the deposits (temperature, duration).

## Acknowledgement

The financial support by Union Miniére (France) is gratefully acknowledged. The authors are indebted to S. Borensztajn for his help in the SEM and EDS analysis of the electrodes surfaces.

## References

1 R.H. Newnham, *J. Appl. Electrochem.* **22** (1992) 116.
2. D. Pavlov and T. Rogachev, *Electrochim. Acta* **31** (1986) 241.
3. F. Hine, Y. Ogata and M. Yasuda, B. *Electrochim.* **4** (1988) 61.
4. D. Butinelli, G. D'Angelo and G. Signorelli, Industria Mineraria, March (1974) 118.
5. I.W. Wark, *J. Appl. Electrochem.* **9** (1979) 721.
6. R.G. Selim and J.J. Lingane, *Anal. Chim. Acta* **21** (1959) 536.
7. J. Mozota and B.E. Conway, *J. Electrochem. Soc.* **128** (1981) 2141.
8. L.D. Burke, *in* 'Electrodes of conductive Metallic Oxides, Part A' (edited by S. Trasatti), (Elsevier, New York, 1980).
9. T. Shimamune, H. Kawauchi, S. Nakatsu, Y. Nishiki and R. Hayashi, *J. Electrochem. Soc.* **89** (1989) 555.
10. G. Lodi, A. De Battisti, G. Bordin, C. De Asmundis and A. Benedetti, *J. Electroanal. Chem.* **277** (1990) 139.
11. R. Kôtz and S. Stucki, *Electrochim. Acta* **31** (1986) 1311.
12. J. Rolewicz, Ch. Comninellis, E. Plattner and J. Hinden, *Electrochim. Acta* **33** (1988) 573.
13. Ch. Comninellis and G.P. Vercesi, *J. Appl. Electrochem.* **21** (1991) 335.
14. G.P. Vercesi, J.Y. Salamin and Ch. Comninellis, *Electrochim. Acta* **36** (1991) 991.
15. V.A. Alves, L.A. Da Silva, J.F.C. Boodts and S. Trasatti, *Electrochim. Acta* **39** (1994) 1585.
16. L.A. Da Silva, V.A. Alves, M.A.P. Da Silva, S. Trasatti and J.F.C. Boodts, *Electrochim. Acta* **42** (1997) 271.
17. J. Krysa, J. Maixner, R. Mraz and I. Rousar, *J. Appl. Elecrochem.* **28** (1998) 369.
18. R.K. Jaworski, J.A. Cox and B.R. Strohmeier, *J. Electroanal. Chem.* **325** (1992) 111.
19. T. Yoshino, N. Baba and K. Arai, *Jap. J. Appl. Phys.* **26** (1987) 1547.
20. D.A.J. Rand and R. Woods, *J. Electroanal. Chem.* **55** (1974) 375.
21. K. Yamanaka, *Jap. J. Appl. Phys.* **30** (1991) 1285.
22. J.E. Baur, T.W. Spaine, *J. Electroanal. Chem.* **443** (1998) 208.
23. M.A. Petit and V. Plichon, *J. Electroanal. Chem.* **444** (1998) 247.
24. C. Cachet, C. Rérolle and R. Wiart, *Electrochim. Acta* **41** (1996) 83.
25. J.E. Ferrer and L.L. Victori, *Electrochim. Acta* **39** (1994) 667.